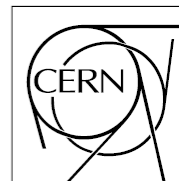


**The Compact Muon Solenoid Experiment**

# **CMS Note**

Mailing address: CMS CERN, CH-1211 GENEVA 23, Switzerland



**3 June 2009**

## **The variation in response of the CMS ECAL vacuum phototriodes as a function of orientation in a strong magnetic field**

R.M. Brown

*STFC Rutherford Appleton Laboratory, Didcot, UK*

### **Abstract**

An analytic model is presented that describes the principle features characterising the behaviour of CMS ECAL vacuum phototriodes in a strong magnetic field. The results are compared with experimental measurements.

## Introduction

The CMS electromagnetic calorimeter (ECAL) is located within the magnetic field volume of the 3.8 Tesla superconducting solenoid. It comprises a barrel section, containing 61200 lead tungstate crystals, and two endcaps, each having 7324 crystals. Scintillation light is registered in photodetectors mounted on the rear face of each crystal. In the barrel section, the chosen devices are avalanche photodiodes (APDs), specially developed by Hamamatsu Photonics for CMS. In the endcaps, where the radiation levels are higher and the magnetic field direction is within  $25^\circ$  of the crystal axes, vacuum phototriodes (VPTs) are deployed. VPTs are photomultipliers with a single gain stage (Fig.1) and these particular devices (FEU188) were specially developed for CMS by RIE, St Petersburg. They have an effective sensitive area of  $280 \text{ mm}^2$ , an average quantum efficiency of  $\sim 20\%$  and a typical gain of 10 in a field of 4 T. The front window is composed of radiation-resistant, UV-transmitting glass.

Although VPTs are relatively insensitive to favourably-oriented, strong magnetic fields, nevertheless the response does vary as a function of field strength and direction. Previous CMS Notes by J.E. Bateman [1] have reported Monte Carlo studies of the magnetic field dependence and comparisons with measurements made on various prototype devices. The purpose of the present Note is demonstrate how magnetic field measurements made on the production VPTs used in CMS may be understood in terms of an analytic model, extended to include the effect of anode grid thickness.

## VPT operation a strong magnetic field

The co-ordinate system is shown in figure 2, with a schematic representation of the VPT electrode structure superimposed. The z-axis is perpendicular to the plane of the page.

The motion of electrons in crossed electric and magnetic fields is characterised by three components [1]:

- (1) uniform acceleration along the x-axis:  $d^2x/dt^2 = (e/m) E \cos(\theta)$
- (2) circular motion around the B direction (x-axis) with radius  $\rho$  and angular frequency  $\omega$ , where  $\rho = \beta/\omega$ ,  $\omega = B(e/m)$  (the electron cyclotron frequency) and  $\beta = E \sin(\theta)/B$ .
- (3) constant drift in the z-direction with velocity  $v_z = \beta$ .

(For simplicity, we have started by assuming the limiting case  $\mathbf{v}(0) = 0$ )

It is instructive to insert some typical numbers at this point:

$$V_C = 0, V_D = 800, V_A = 1000.$$

$$d_{AD} = 2 \text{ mm}, \rightarrow E_{AD} = 10^5 \text{ V m}^{-1}.$$

$$B = 4 \text{ T}.$$

$$\text{Then } \beta = 2.5 \times 10^4 \sin(\theta) \text{ m s}^{-1}$$

$$\omega = B \times 1.76 \times 10^{11} \text{ rad s}^{-1} = 0.704 \times 10^{12} \text{ rad s}^{-1}$$

$$\rho = 0.035 \sin(\theta) \mu\text{m}$$

A critical parameter in determining the behaviour of the VPT in a strong magnetic field is the 'pitch' of the anode grid,  $p$  (see Fig 2.).

The value [2] of  $p$  for the FEU-188 devices is  $10 \mu\text{m}$  ('100 lines per mm'). Thus we see that in the limiting case,  $\mathbf{v}(0) = 0$ , the cyclotron radius at 4 T is very much smaller than  $p$ .

Since  $\mathbf{v}(0) = 0$  is a good approximation for the emission of photoelectrons from the photocathode, the Anode grid casts a sharp shadow on the Dynode, limiting the points of

origin of the secondary electrons. If we consider the case  $\theta = 0$ , (VPT axis parallel to  $\mathbf{B}$ ) and further assume that the secondary electrons are emitted with zero velocity, then they tend to retrace the path of the incident photoelectrons and pass through the same apertures of the grid. This naïve approximation therefore predicts that the VPT response will be zero for  $\theta = 0$ .

The reason the response does not fall to zero (although there is a **dip** at  $\theta = 0$ ), is that the secondary electrons do not have  $\mathbf{v}(0) = 0$ . For  $\theta = 0$ , the cyclotron radius  $\rho = v_T(0)/\omega$ , where  $v_T$  is the ‘transverse velocity’  $v_T = \sqrt{v_y^2 + v_z^2}$ . In the case (for example) of an electron emitted with a kinetic energy of 10 eV at  $30^\circ$  to the tube axis,  $v_T = 10^6 \text{ m s}^{-1}$  and  $\rho = 1.4 \text{ }\mu\text{m}$ , giving a significant probability that the secondary electron will strike the Anode grid.

It is clear from this that the form of the secondary emission spectrum as a function of energy and angle is important in determining the detailed angular dependence of the VPT response. There is extensive literature on this subject (see for example [1,3] and references therein). The energy spectrum (see for example [4]), figure A1.11) has a low energy peak at a few eV, extending to a few tens of eV (secondary emission), in addition there is a narrow high energy peak close to the incident energy (back-scattered electrons) and between the two there is a low plateau (primary electrons suffering multiple inelastic collisions).

The angular distribution of the secondary electrons has a  $\cos(\theta)$  dependence centred on the normal to the Dynode surface (and therefore independent of the incident electron direction with respect to the plane of the Dynode.).

### Dip structure

We consider first the effect on the angular distribution of component (3) above, the constant velocity drift in the z-direction (normal to the  $\mathbf{E} \times \mathbf{B}$  plane). This gives rise to a displacement that increases linearly with time. Thus in the limit  $v_z(0) = 0$ :

$$z(t) = (E \sin(\theta)/B) t$$

In the case of the secondary electrons, the z-displacement when they reach the Anode is proportional to the time,  $t_f$ , taken to cross the Anode-Dynode gap. Integrating (1), (and setting  $z(0) = 0$ ,  $\mathbf{v}(0) = 0$ ):

$$x(t_f) = (1/2) (e/m) E \cos(\theta) t_f^2$$

thus since  $x(t_f) = d_{AD} / \cos(\theta)$ :

$$t_f^2 = 2 (m/e) (d_{AD}/E_{AD}) / \cos^2(\theta)$$

(**Note** that this expression differs by a factor  $1/\cos(\theta)$  compared to the corresponding expression in reference 1.)

$$\text{Thus } t_f = d_{AD} \sqrt{[2m/(e(V_A - V_D))]} / \cos(\theta)$$

$$\text{and } z(t_f) = \sqrt{[2(V_A - V_D)(m/e)]} \tan(\theta) / B$$

For  $(V_A - V_D) = 200 \text{ V}$ ,

$$z_{se}(t_f) = (47.6/B) \tan(\theta) \text{ }\mu\text{m}$$

(Note that this should be considered as the maximum z-displacement, since secondary electrons emitted with non-zero velocity will take less time to cross the Anode-Dynode gap.)

The points of origin of the secondary electrons also suffer a displacement in  $z$  as  $\theta$  is varied, since the shadow of the grid, cast on the Dynode by the photoelectrons, moves. Since the displacement depends on  $E/B$  and not on the sign of the velocity, it is in the same direction as the displacement of the secondary electrons. The photoelectrons are accelerated to an energy  $eV_A$  when they reach the anode, thus they enter the Anode-Dynode gap with a velocity proportional to  $\sqrt{V_A}$ . They then decelerate and strike the Dynode with a velocity proportional to  $\sqrt{V_D}$ . It may be shown that  $t_f(\text{pe})$  is obtained by replacing  $\sqrt{1/(V_A - V_D)}$  in the expression for  $t_f(\text{se})$ , by  $\sqrt{1/((V_A + V_D) + 2\sqrt{V_A V_D})}$ , leading to an additional displacement:

$$z_{\text{pe}}(t_f) = (11.2/B) \tan(\theta) \mu\text{m}.$$

The total change in the mean  $z$ -position of the secondary electrons at the Anode is thus given by  $[z_{\text{se}}(t_f(\text{se})) + z_{\text{pe}}(t_f(\text{pe}))]$ .

At first sight, it might be expected that this  $\theta$ -dependent displacement in  $z$  would give rise to the observed structure in the response, with dips occurring at values of  $z(t_f)$  equal to multiples of the grid pitch,  $p$ . However, the fact that the dip in response at  $\theta = 0$  is relatively shallow demonstrates that the randomising effect arising from the spread in transverse velocities of the emitted secondary electrons will wash out a contribution to the peak/dip structure arising from the  $z$ -drift in the Anode-Dynode region.

In fact the probabilities for a secondary electron to strike the grid mesh or to pass through an aperture in the grid depend principally on the grid transmission,  $T'$ , described in the next section. It turns out that it is the fate of that proportion  $T'$  of the secondary electrons that passes through the grid on the first traversal that dominates the dip structure.

Secondary electrons escaping capture on the Anode decelerate in the Cathode-Anode field and then accelerate back to the plane of the grid. In the limit that the secondary electrons are emitted with  $\mathbf{v} = 0$  (contradicting the randomisation argument – but nevertheless a reasonable approximation!), then their behaviour in the Cathode-Anode gap just mirrors that in the Dynode-Anode gap. Thus the  $z$ -drift up to the point where the electron comes to rest in the Cathode-Anode gap is equal to that calculated above for the drift in the Dynode-Anode gap.

(Note that although the field is  $\sim 3.3$  times higher in the Cathode-Anode gap than in the Dynode-Anode gap (assuming a Cathode-Anode spacing of 3 mm, a Dynode-Anode spacing of 2 mm and  $V_A = 1000$ ,  $V_D = 800$ )), the time spent in the gap is correspondingly less and the effect of the higher field cancels in the expression for  $z(t_f)$ .

As the electrons accelerate back towards the Anode, they undergo a further drift in  $z$  of the same magnitude and the same sign. The total drift experienced between the initial traversal of the grid and the return to the grid is thus:

$$z_{\text{se}}(t_f) = (95.2/B) \tan(\theta) \mu\text{m}$$

Thus dips in response occur at angles  $\theta_n$  where  $z_{\text{se}}(t_f)$  has a value that is an integer multiple of the grid pitch:

$$\tan(\theta_n) = (n p B)/95.2 \quad \text{where } p \text{ is the pitch.}$$

For  $p=10 \mu\text{m}$  :

$$\theta_1(3.8 \text{ T}) = 21.8^\circ, \quad \theta_1(1.8 \text{ T}) = 10.7^\circ, \quad \theta_1(0.9 \text{ T}) = 5.4^\circ$$

- in good agreement with observation (figure 3). The red arrows indicate the predicted positions of the first dips, relative to the measured position of the central dip.

### The effect of Anode grid thickness.

Figure 4 (left) shows a 3-dimensional representation of the Anode grid structure. In addition to the pitch, the grid is characterised by an ‘aperture’ (a) and a ‘thickness’ (t). An important property of the grid is its ‘transparency’ (T), where:

$$T = (a/p)^2$$

It may be noted that the dip structure of the VPT response as a function of angle, discussed above, is insensitive to the grid thickness. This is because the z-component of the angle between the secondary electron directions and the normal to the grid, caused by the z-drift, is always very small. However, the grid thickness does have a strong effect on the **overall** angular dependence of the tube response.

As T is increased, the probability for a photoelectron to reach the Dynode increases, however, the probability for a secondary electron to be captured by the Anode decreases. If the two probabilities are uncorrelated, then the tube response varies as  $[T \times (1-T)]$  and is maximised for  $T = 0.5$ . Evidence that the two probabilities are indeed no more than weakly correlated is given by the shallow nature of the dip in response at  $\theta = 0$ .

It is clear that the effective transparency of the grid will decrease as  $\theta$  is increased. From figure 4 (right) it can be seen that at an angle  $\theta$ , the effective transparency becomes:

$$T' = (a/p) (a'/p') \quad \text{where: } a' = [a \cos(\theta) - t \sin(\theta)] \quad \text{and } p' = p \cos(\theta)$$

$$\text{Thus: } T' = (a/p)^2 [1 - (t/a) \tan(\theta)]$$

The relative tube response changes from  $[T \times (1-T)]$  at zero angle, to  $[T' \times (1-T')]$  at angle  $\theta$ . (Neglecting the effect of the change in capture probability for secondary electrons would lead to a predicted change in tube response from T to T').

Figure 5 compares the measured tube response as a function of angle, with the predictions of both a T-dependence and a  $[T \times (1-T)]$  -dependence. It is clear that the increase in the capture probability for secondary electrons, with increasing  $\theta$ , must be taken into account in order to obtain satisfactory agreement with the data. The results are consistent with a thickness of the Anode grid of  $2.75 \mu\text{m}$ .

### The effect of grid orientation

Finally, it is important to note that so far, we have only considered the case where the tube rotation relative to the magnetic field direction is in a plane that contains one of the grid ‘axes’. In the case where the plane of rotation is at an angle ( $\phi$ ) of  $45^\circ$  to one or other of the grid axes, the effective grid pitch becomes  $p\sqrt{2}$  and the effective aperture becomes  $a\sqrt{2}$  in the planes parallel to and normal to the plane of rotation, but the effective thickness t is unchanged.

The effect on the dip structure at a given B-field is an increase by  $\sqrt{2}$  in the values of  $\tan(\theta)$  for which dips occur. This can be seen in figure 6 (top), which compares curves of  $\theta$ -dependence measured for two values of  $\phi$ :  $0^\circ$  and  $45^\circ$ . (One of the  $\phi = 45^\circ$  curves has been offset in y by 0.1 for clarity.) Rescaling the  $\theta$  values ( $\theta \rightarrow \tan^{-1}(\tan(\theta)/\sqrt{2})$ ) results in an alignment of the dips observed in the two  $\theta$  distributions. (As an aside, it is interesting to note that there is a small but visible residual misalignment of the second dip if  $\theta$ , rather than  $\tan(\theta)$ , is rescaled.) Figure 6 (bottom) shows the  $\theta$ -dependence of the response for two  $\phi$  values in a field of 3.8 T.

The effect on the overall angular dependence is expected to be an extension of the response plateau by  $10^\circ$  on either side. (This prediction has not been checked.)

### **Summary**

The VPTs used in the ECAL endcaps of CMS show a systematic variation of response as a function of orientation with respect to the direction of an applied magnetic field. The main features (dip structure, fall off at large angles) may be understood in the framework of an analytic model that takes into account the pitch and the thickness of the anode grid.

### **Acknowledgements**

The experimental results included in this Note were obtained by groups at the Rutherford Appleton Laboratory and the University of Virginia. Their efforts are gratefully acknowledged.

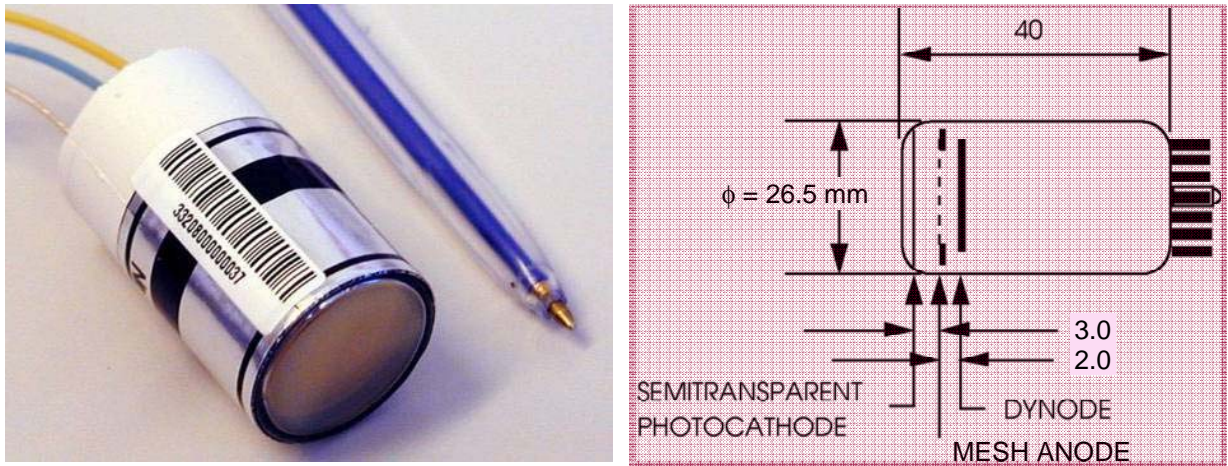


Figure 1: The vacuum phototriode used in the CMS ECAL endcaps

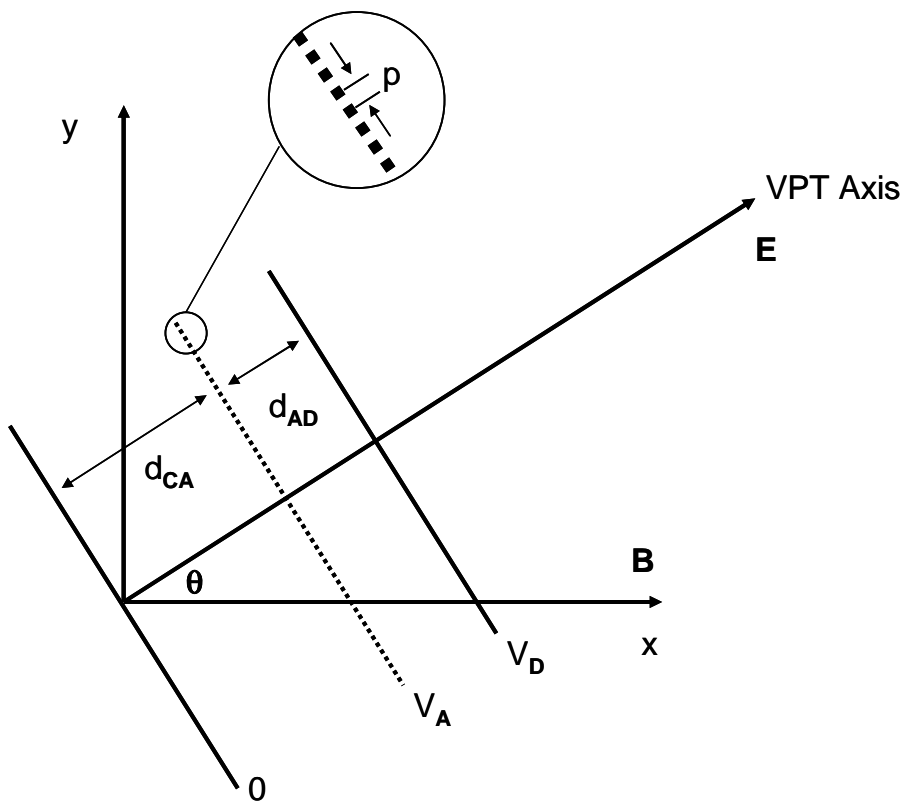


Figure 2: The coordinate system with a schematic representation of the electrode structure superimposed

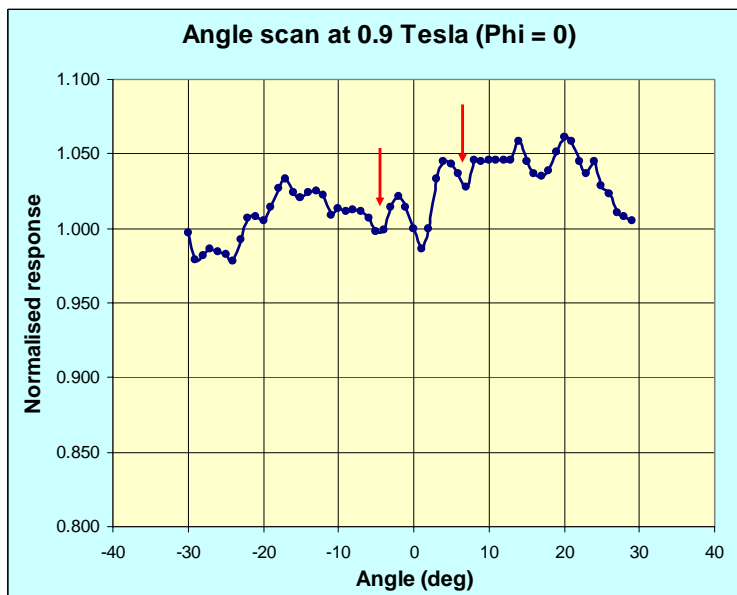
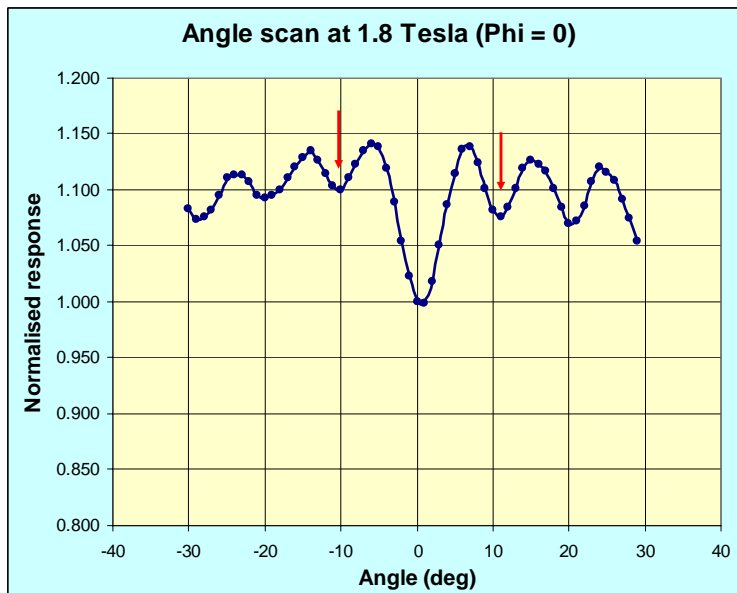
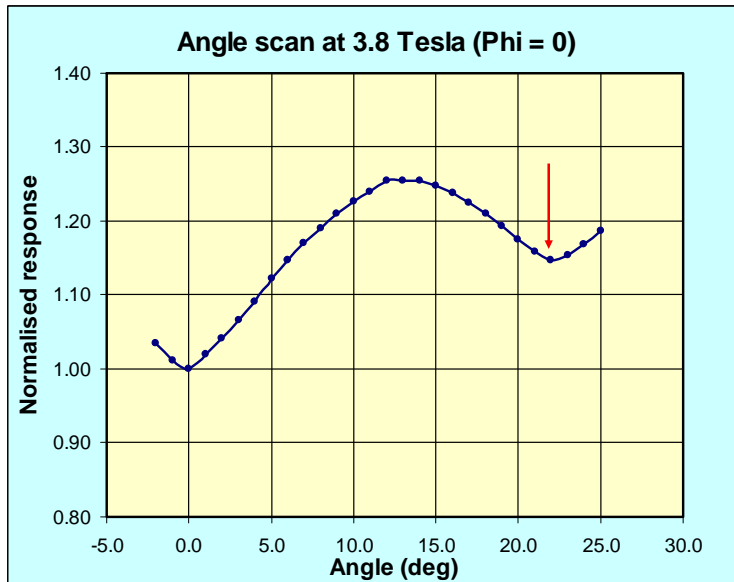


Figure 3: The relative response as a function of angle (orthogonal alignment of grid).  
 Top: 4.0 Tesla; Centre 1.8 Tesla; Bottom 0.9 Tesla

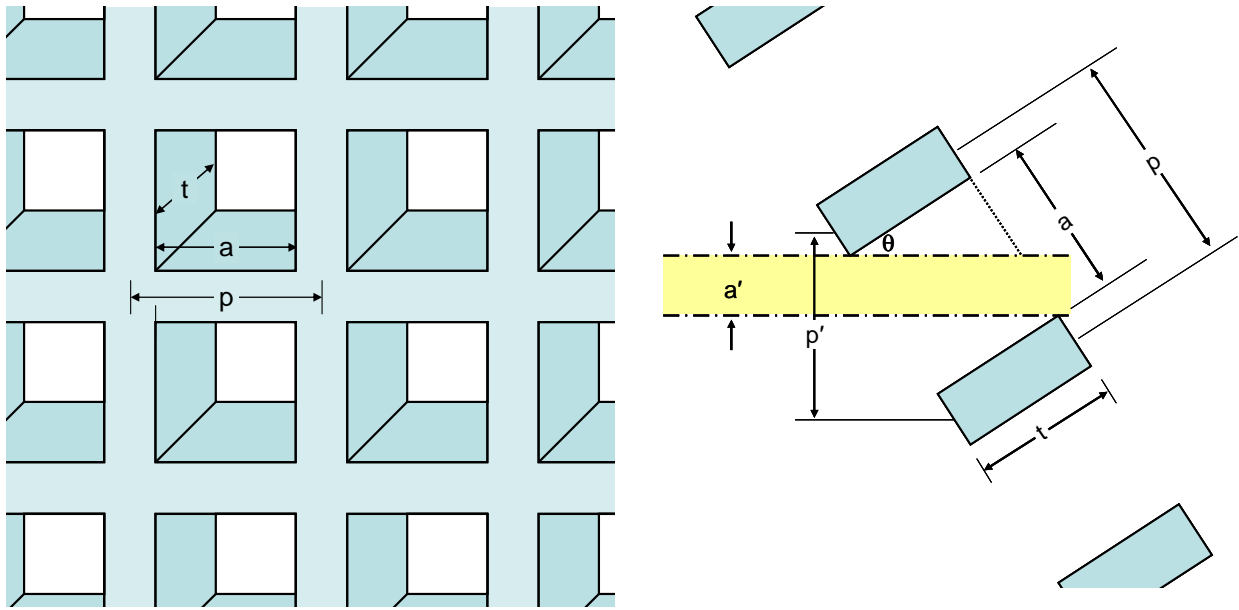


Figure 4: Left: A schematic representation of the Anode grid  
 Right: The effect of the tilt angle on the effective grid aperture

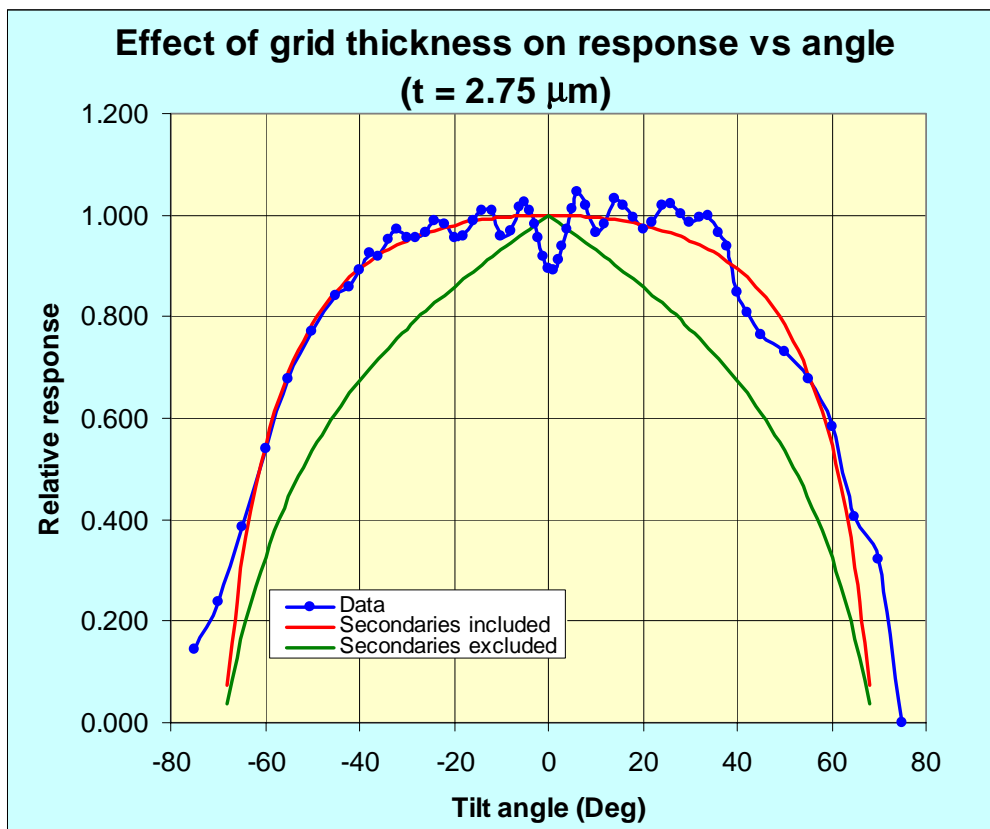


Figure 5: The effect of Anode grid thickness on the angular dependence of the response

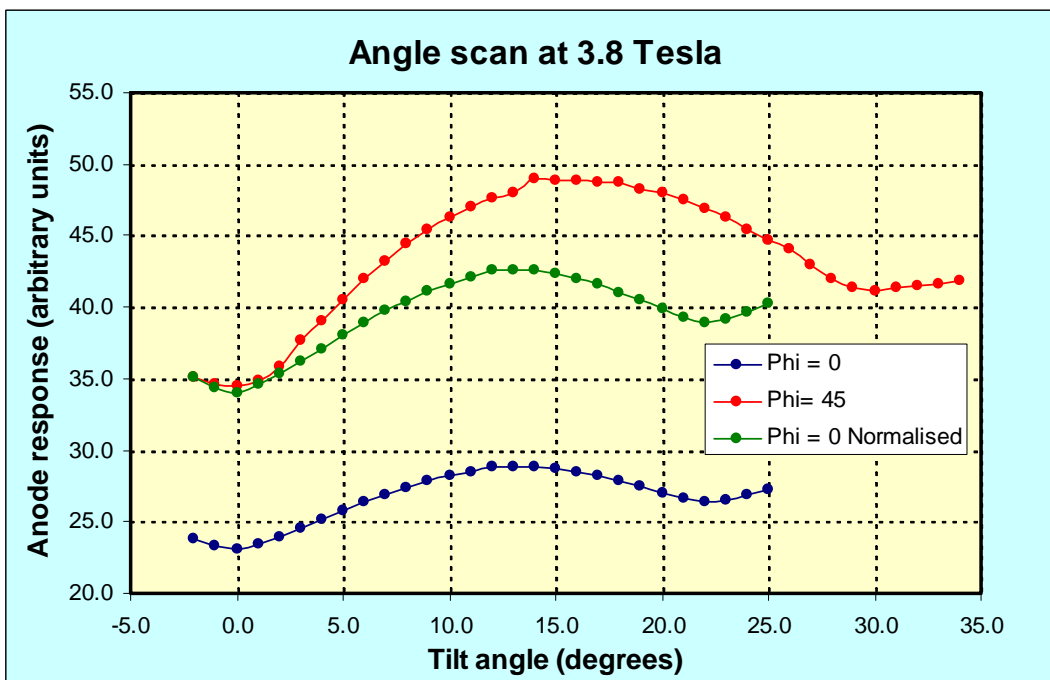
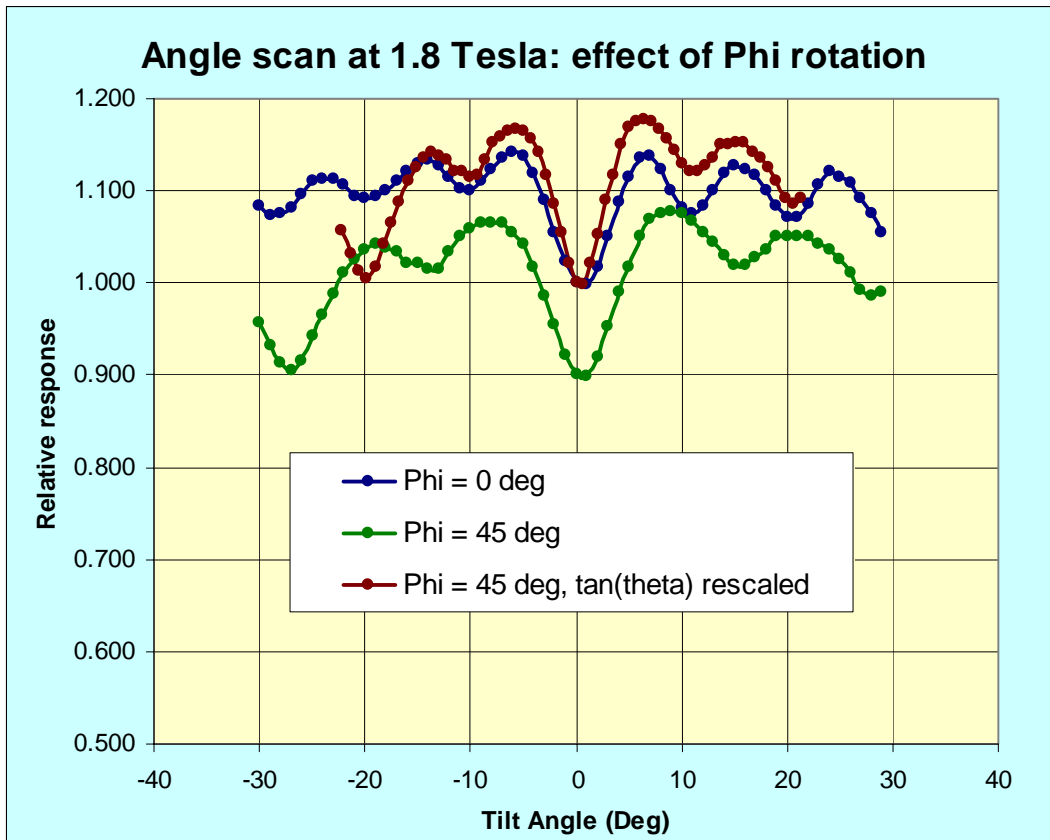


Figure 6: The effect of the grid orientation,  $\phi$ , on the angular dependence of the response  
 Top: 1.8 Tesla. Bottom: 3.8 Tesla.

- 
- 1 E.Bateman, CMS Note 1998/059, CMS Note 1999/032
  - 2 Super Radiation Hard Vacuum Phototriodes for the CMS Endcap ECAL, Yu.I. Gusev et al.
  - 3 Secondary electron emission due to primary and backscattered electrons, K. Kanaya and H. Kawakatsu, J. Phys. D: Appl. Phys., Vol. **5**, 1972.